

Hydrodynamic Dispersion of Noncolloidal Suspensions: Measurement from Einstein's Argument

J. Martin, N. Rakotomalala, and D. Salin

Laboratoire Acoustique et Optique de la Matière Condensée, Université Pierre et Marie Curie, Case 78, 4 Place Jussieu, 75252 Paris, Cedex 05, France*
and Laboratoire Fluides, Automatique et Systèmes Thermiques, Batiment n°502 Campus Universitaire, 91405 Orsay Cedex, France*

(Received 7 July 1994)

Following Einstein's argument for the diffusion coefficient of colloidal dispersions, we postulate that the steady state concentration profile in a suspension of noncolloidal monodisperse particles reflects the dynamic equilibrium resulting from a balance between gravity-driven convection and hydrodynamic dispersion. Using an acoustic technique, the steady state concentration profile of a counterflow-stabilized suspension (a fluidized bed) as well as stationary propagating sedimentation fronts inside the bed were determined. From these profiles we can derive the concentration dependence of the hydrodynamic dispersion coefficient.

PACS numbers: 47.15.Pn, 05.40.+j, 47.35.+i

In a colloidal suspension, the particles are small enough to perform Brownian motions: The movements of the individual particles give rise to a diffusion process due to stochastic thermal fluctuations. When the particles are large enough, hydrodynamic interactions between particles prevail over Brownian motion. In such a noncolloidal suspension of volume fraction C , the velocity of an individual particle fluctuates about the mean settling velocity $U(C)$. These fluctuations lead to a random walk of the particles, due to the hydrodynamic interactions with the surrounding particles. This diffusion process is referred to as hydrodynamic dispersion [1–5]. Experimental observations of shear-induced diffusion [1], broadening of the interface at the top of a sedimenting suspension [2], and velocity fluctuations of a single particle in the bulk of a sedimenting homogeneous suspension [3] support this idea of hydrodynamic dispersion of a noncolloidal suspension of monodisperse particles [4,5]. Accurate experiments [6,7] and theoretical understanding [4,8] of this phenomenon are still a challenge. Measurements of the hydrodynamic dispersion coefficient $D(C)$ have been obtained by two different approaches. The first relies on tracking the velocity fluctuations either of a tagged particle settling among and being part of a homogeneous suspension [3,9] or of the whole suspension [6]; the variance of these fluctuations leads to D . The second relies on analyzing the large concentration gradient occurring at the top of a sedimenting suspension, the front spreading due to hydrodynamic dispersion [2,7,10]. Note that the two methods actually address two different dispersion issues, namely, self-diffusion in the former and the collective response of the suspension to a concentration gradient in the latter. Both methods have intrinsic experimental limitations: The first requires a reproducible stirring procedure in order to obtain homogeneous suspensions, while the second is affected by even small residual polydispersity (which leads to a

growth proportional to time t) which rapidly overcomes the dispersion effect (which grows as $\sim\sqrt{t}$). A suitable tool to avoid such sedimenting suspension problems is to employ a fluidized bed, in which case the upward-flowing solvent counterbalances gravity. Thus the “settling” concentration profile reaches a steady state, with respect to a laboratory frame of reference, in which case accurate measurements can be performed [6]. Moreover, by virtue of the fluidization process (which leads to segregation, with smaller particles at the top and larger at the bottom) the bed intrinsically discriminates between small and large particles, thereby overcoming polydispersity problems. Such a system was recently used [6] to measure the properties of a colloidal suspension, although the suspension was assumed to have a uniform concentration contradicting recent measurements in charged-particle systems [11]. To detect the sharp concentration variations of the concentration profile requires an accurate technique with a well designed spatial resolution. In this Letter, we use an acoustic technique [12] to obtain measurements of the concentration profile in a liquid-fluidized bed of noncolloidal particles. Applying a phenomenological extension of Einstein's derivation [13] of the diffusion coefficient of a colloidal suspension to the profiles of our noncolloidal system, we determine the concentration dependence of the hydrodynamic coefficient.

Let us first recall some basic aspects of suspensions and fluidized beds [4]. We consider a collection of monodisperse spherical particles fluidized in a liquid. The particles are large enough for Brownian motion to be negligible. For a suspension statistically homogeneous in each horizontal direction, the volume fraction $C(x, t)$ is a function of the vertical direction x (downward oriented) and time t . The mean velocity of the suspension is $V = CV_p + (1 - C)V_f$, where V_p and V_f are the particle and fluid velocities, respectively (all velocities are algebraic quantities). In the absence of inertia and

concentration gradients, the momentum equation gives [4] $V_p - V = U(C)$, which expresses the balance between viscous and buoyancy forces [$U(C) = M(C)V_0$, where $M(C)$ is the concentration-dependent friction and $V_0 = 2a^2(\rho_p - \rho_f)g/9\eta$ is the Stokes sedimentation velocity of a single spherical particle of radius a , with η the viscosity, g the acceleration of gravity, and ρ_p and ρ_f the particle and fluid densities]. When concentration gradients exist, the equation must be modified to account for the hydrodynamic dispersion. Following Einstein's argument [13] for the determination of the diffusion coefficient of colloidal dispersions, we postulate that the steady state concentration profile in a suspension of noncolloidal monodisperse particles reflects the dynamic equilibrium resulting from a balance between gravity-driven convection and hydrodynamic dispersion. Therefore we express the particle flux $J = CV_p$, as the sum of a convective and diffusive flux, to get

$$CV_p = C(U(C) + V) - D(C)\nabla C. \quad (1)$$

Substitution in the equation for the conservation of particles, $\partial C/\partial t + \partial J/\partial x = 0$, yields the convection-diffusion equation

$$\partial C/\partial t + \partial[C(U(C) + V)]/\partial x = \partial[D(C)\partial C/\partial x]/\partial x. \quad (2)$$

In a steady state in the laboratory frame of reference ($\partial C/\partial t = 0$, $V = -q$, where q is the volume-fraction injection velocity), we further get

$$C[U(C) - q] = D(C)\partial C/\partial x, \quad (3)$$

where the integration constant was set to zero as required by the far-field boundary condition. Equation (3) expresses the fact that the net convective flux due to an external force (gravity) through a plane moving at the suspension velocity is counterbalanced by the diffusion flux. This is the basic Einstein argument we used to derive the diffusion coefficient of a colloidal suspension [13]. The concentration profile $C(x)$ can be obtained from integration of Eq. (3), provided that $U(C)$ and $D(C)$ are known. This is the same stationary shape profile that should be observed at the top of a sedimenting suspension [10], if polydispersity effects are negligible. Note that at steady state the concentration in the uniform concentration region and the flow rate are related by $U(C) = q$.

Experiments were performed in a column 60 cm high of circular cross section (4 cm). We determined the concentration profile by measuring variations in the sound speed in several cross sections along the bed, as the sound speed in suspensions is related to the volume fraction of particles [12]. From the calibration curve and the accuracy of our relative velocity measurements (10^{-4}) we estimated [12] the overall accuracy in concentration measurements to be 0.1% and the spatial resolution to be 1 mm. The liquid used was a water-glycerol mixture ($\eta = 2 \times 10^{-3}$ SI units). The spherical glass beads had

diameter $2a = 68.5 \mu\text{m}$, with 95% of the particles in the range 63–74 μm . In the experiments, the particle Reynolds number ($\text{Re} = V_0 a \rho_f / \eta$) was less than 0.1, while Brownian motion was negligible ($kT/6\pi\eta a^2 V_0 < 10^{-7}$).

Figure 1 shows a typical concentration profile $C(x)$ and its gradient $\partial C/\partial x$, for a flow rate corresponding to an average concentration of $C_0 \sim 22\%$. The profile consists of two parts, a top front of extent L , where the concentration increases from 0 to nearly C_0 , and a long tail where the concentration is nearly constant ($\sim C_0$). As expected, the bulk of the bed is uniform at C_0 . Using different flow rates q , we can determine the relation $U(C)$. In agreement with previous authors [6,9], we find the result $U(C) = V_0(1 - C)^p$ with $p \sim 5.0 \pm 0.2$. Subsequently, using the measured values of C and $\partial C/\partial x$, we can deduce the hydrodynamic coefficient $D(C)$ from (3). Figure 2 is a plot of the normalized coefficient $D(C)/aU(C)$ (filled squares). It must be noted that the smaller the flow rate, the sharper the front, making the measurements more difficult. Such a sharpening is expected from an inspection of Eq. (3): For a fixed flow rate $q = U(C_0)$, the maximum gradient is of the order C_0/L , or writing $D(C) = naU(C)$, then $L \sim na/C_0$ ($n \sim 50$). For $C_0 = 10\%$, L is of the order of 2 cm. Thus, larger concentrations require the design of a different experimental procedure that yields larger front widths.

In the following, we shall take advantage of both sedimenting suspension and fluidized bed features: The bed provides a steady homogeneous suspension in its bulk; reducing the flow rate abruptly from $q_1 = U(C_1)$ to $q_2 = U(C_2)$, a relative sedimentation is expected to occur, from C_1 to C_2 ($C_1 < C_2$), with a front propagating from bottom to top. As the settling velocity $U(C)$ is a decreasing function of concentration, smaller concentrations fall faster than larger ones, leading to a sharp (self-sharpening [14]) shock front. Because self-sharpening

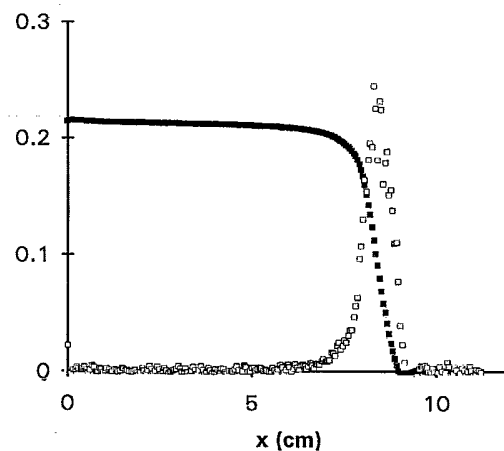


FIG. 1. Concentration (■) and concentration gradient (□) versus vertical position x along the fluidized bed (bottom of the bed is at the right).

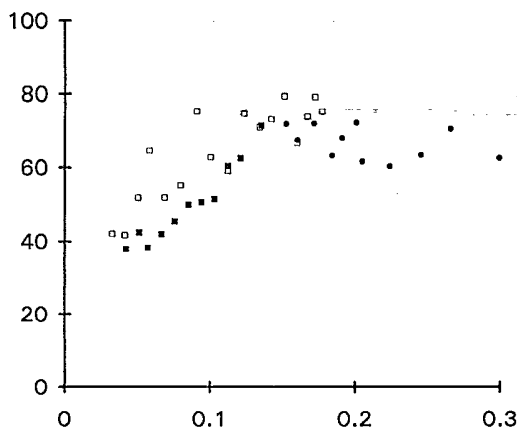


FIG. 2. Concentration dependence of the normalized hydrodynamic dispersion coefficient $D(C)/aU(C)$: from the steady state concentration profile, Fig. 1 (■), the sedimenting stationary top front (□), and from the stationary propagating sedimentation fronts, Fig. 3 (●).

and hydrodynamic dispersion have opposing effects, this leads to a stabilized dispersed profile which propagates at a constant velocity V_s without changing its shape [note that Eq. (2) is a Burger's type equation [10,15]]. We can obtain traveling wave solutions of Eq. (2) of the form $C(X)$, $X = x - V_s t$, where $C(X)$ is the solution of $C[U(C) - q - V_s] = D(C)\partial C/\partial X + A$. The two constants A and V_s are determined by the far-field conditions, where the concentration tends to C_1 and C_2 , respectively, and the concentration gradients vanish. Thus, $V_s = C_1(q_2 - q_1)/(C_2 - C_1)$, while the stationary profile follows from

$$(C_2 - C_1)D(C)\partial C/\partial X = (C_2 - C)[F(C) - F(C_1)] + (C - C_1)[F(C) - F(C_2)], \quad (4)$$

where we denoted $F(C) = CU(C)$. Note that in such a relative sedimentation the front width scales as $L \sim na/(C_2 - C_1)$, showing that we can choose the appropriate width provided that self-sharpening still occurs [10,15]. As particles slow down across the front, additional phenomena such as inertia and particle velocity gradient come into play [4,6]. In the following, high-concentration data analysis required us to take into account particle viscosity effects, a complete description of which will be postponed until a forthcoming paper. For example, in the experiment, if we reduce the flow rate, the previous steady state profile propagates, stationary, but with a slightly different shape indicating an increase of the dispersion coefficient, related most likely, to inertia effects (in Fig. 2, open squares are above filled squares).

Figure 3 shows the concentration variation as a function of time, versus the variable X , at two different positions in the bed for an abrupt decrease of the flow rate from q_1 to q_2 , corresponding to $C_1 \sim 15\%$ and $C_2 \sim 33\%$. It is seen that the shape of the profiles is identical at the

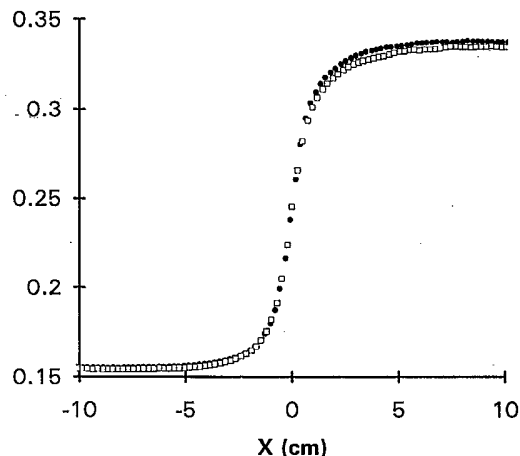


FIG. 3. Time evolution of profiles (concentration versus relative space $X = x - V_s t$) at two positions in the bed, (●) $x_1 = 10$ and (□) $x_2 = 13$ cm, from the bottom, corresponding to an abrupt decrease of the flow rate: The concentration shapes are translationally invariant and correspond to a stationary propagating sedimentation front.

two different locations, indicating a traveling front, the velocity of which was determined to be constant and its value in agreement with the above prediction. This is the first observation of a stationary propagating front in a sedimenting suspension. Moreover, the equilibrium character of this stationary front can be tested: Instead of an abrupt jump we decrease the flow rate with a ramp leading to an apparent concentration profile width λ ; if λ is smaller than the stationary front width L , the front spreads upward until it reaches the L value, whereas for λ larger than L , the front sharpens upward to L . Using the same procedure as above, but using Eq. (4) now, we can measure the diffusion coefficient, whose values we plot in Fig. 2 (filled circles). In the overlapping region both experimental methods give D values in reasonable agreement. Our data clearly show that $D(C)/aU(C)$ increases roughly linearly with the volume fraction up to 15% and is almost constant in the range 15–30%; it vanishes when the concentration approaches the packing one ($\sim 60\%$). The scattering of each data set leads to an overall accuracy of 10% in D , but we have not used any kind of data fit to derive the concentration gradient (Fig. 1). Note that the D determination is controlled by the knowledge of not only the flux $F(C)$, but its derivatives. Thus for concentration jumps around a concentration of 35%, the D determination is not very precise but the trend is there. Large concentrations, as well as the very low ones, will require more experimental effort. We point out that the low concentration values of D are almost three times as large as those previously determined from sedimentation front broadening [2,7,10]. And although in our experiments the Reynolds number (0.1) is larger than that in the previous determinations (10^{-3}), the normalized dispersion coefficient remains

the same when it is decreased, indicating that viscous forces are dominating. The values found are twenty times larger than those reported [3,8,9], based on the velocity fluctuations of a single particle or of the whole suspension [6]. This supports the contention that the latter measurements only capture the self-diffusion part of hydrodynamic dispersion.

Using an acoustic technique, we have measured the steady state concentration profile of a liquid-fluidized bed of monodisperse noncolloidal particles. Extending Einstein's argument on the derivation of the diffusion coefficient of a colloidal dispersion, we have measured the hydrodynamic dispersion coefficient of this noncolloidal suspension. To reach a relatively large concentration range we have used our fluidized bed in a relative sedimentation regime and have observed propagating sedimentation fronts and traveling waves inside this bed. These two techniques allow for controlling the front width and also for determining the concentration dependence of the hydrodynamic dispersion coefficient over a large range of concentration.

This paper has benefited from stimulating discussions with Professor G. M. Homsy, Professor D. Lhuillier, and Professor Y. C. Yortsos. It is a pleasure to acknowledge the financial support of GDR, CNRS Physique des Milieux Hétérogènes Complexes.

*Associated with the Centre National de la Scientifique.

- [1] D. Leighton and A. Acrivos, *J. Fluid Mech.* **177**, 109 (1987); **181**, 415 (1987).
 [2] R. H. Davis and K. H. Birdsell, *AIChE. J.* **34**, 123 (1988);

- R. H. Davis and M. A. Hassen, *J. Fluid Mech.* **196**, 107 (1988).
 [3] J. Ham and G. M. Homsy, *Int. J. Multiphase Flow* **14**, 533 (1988); J. Ham, S. Thomas, E. Guazzelli, and G. M. Homsy, *Int. J. Multiphase Flow* **16**, 171 (1990).
 [4] G. K. Batchelor, *J. Fluid Mech.* **52**, 245 (1972); **193**, 75 (1988).
 [5] R. E. Catfish and J. H. C. Luke, *Phys. Fluids* **28**, 759 (1985).
 [6] J. Z. Xue, E. Herbolzheimer, M. A. Rutgers, W. B. Russel, and P. M. Chaikin, *Phys. Rev. Lett.* **69**, 1715 (1992), and references therein; *Fluidization*, edited by J. F. Davidson, R. Cliff, and D. Harrison, (Academic Press, London, 1985).
 [7] S. Lee, Y. Jang, C. Choi, and T. Lee, *Phys. Fluids A* **4**, 2601 (1992).
 [8] A. J. C. Ladd, *Phys. Fluids A* **5**, 299 (1993), and references therein.
 [9] H. Nicolai, B. Herzhaft, E. J. Hinch, L. Oger, and E. Guazzelli (to be published).
 [10] J. Martin, N. Rakotomalala, and D. Salin, *Phys. Fluids Lett.* **6**, 3215 (1994).
 [11] R. Piazza, T. Bellini, and V. Degiorgio, *Phys. Rev. Lett.* **71**, 4267 (1993).
 [12] D. Salin and W. Schön, *J. Phys. Lett.* **42**, L-477 (1981); J.-C. Bacri, C. Frenois, M. Hoyos, R. Perzynski, N. Rakotomalala, and D. Salin, *Europhys. Lett.* **2**, 123 (1986); J.-C. Bacri, M. Hoyos, N. Rakotomalala, D. Salin, M. Bourlion, G. Daccord, R. Lenormand, and A. Soucemanianadin, *J. Phys. III (France)* **1**, 1455 (1991).
 [13] A. Einstein, *Ann. Phys. (Leipzig)* **19**, 371 (1906).
 [14] G. J. Kynch, *Trans. Faraday Soc.* **48**, 166 (1952).
 [15] G. B. Whitham, *Linear and nonlinear waves* (John Wiley and Sons, New York, 1974).